Heliyon 10 (2024) e37430

Contents lists available at ScienceDirect

Heliyon

journal homepage: www.cell.com/heliyon

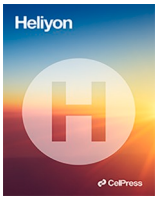

Research article

A central composite design-based targeted quercetin nanoliposomal formulation: Optimization and cytotoxic studies on MCF-7 breast cancer cell lines

E. Bhargav [a], Nawaz Mohammed [a], Udit Narayan Singh [a], P. Ramalingam [b], Ranadheer Reddy Challa [c], Bhaskar Vallamkonda [d], Sheikh F. Ahmad [e], Prasanth DSNBK [f], Praveen Kumar Pasala [a,**], Mithun Rudrapal [g,*]

[a] *Raghavendra Institute of Pharmaceutical Education and Research, Anantapur, Andhra Pradesh, India*
[b] *Department of Pharmaceutical Analysis, National Institute of Pharmaceutical Education and Research (NIPER), Hajipur, Bihar, India*
[c] *Formulation and Development, Quotient Sciences, 3080 McCann Farm Dr, Garnet Valley, PA, USA*
[d] *Somerset Therapeutics Limited, New Jersey, USA*
[e] *Department of Pharmacology and Toxicology, College of Pharmacy, King Saud University, Riyadh-11451, Saudi Arabia*
[f] *School of Pharmacy & Technology Management, SVKM's Narsee Monjee Institute of Management Studies (NMIMS), Jadcherla, Hyderabad, India*
[g] *Department of Pharmaceutical Sciences, School of Biotechnology and Pharmaceutical Sciences, Vignan's Foundation for Science, Technology & Research, Guntur, Andhra Pradesh, India*

ARTICLE INFO

Keywords:
Quercetin
Central composite design
Nanoliposomes
Breast cancer
Cytotoxic

ABSTRACT

This study aimed to enhance the efficacy of quercetin (QT) by formulating it into a liposomal drug delivery system utilizing the concept of central composite design. The drug:lipid ratio, cholesterol concentration, and sonication time were selected as independent variables in the study. The vesicle and percentage entrapment efficiency were selected as the dependent variables. Quercetin nanoliposomes (QT-NLs) were prepared via a combination of ethanol injection and thin film hydration. The vesicle size and entrapment efficiency of all formulations were within the ranges of 100 nm and >80 %, respectively. The zeta potential value indicated the stability of the optimized formulation. The contour plots were used to select the desired batch range. SEM studies revealed an imperfect crystalline morphology without any unwanted agglomeration. MTT assays on VERO cell lines indicated the safety of the developed formulation. MTT assays of MCF-7 cells revealed IC_{50} values of 5.8 μM and 7.9 μM for QT-NLs and QT, respectively. In our study, the optimized formulation exhibited late and early apoptosis and necrosis when used to treat MCF-7 cells. S and G2/M cell cycle phases of MCF-7 cell arrest were confirmed by the cell cycle report. At sub-G0/G1 phase, 2.10 ± 1.1 %; G0/G1 phase, 34.13 ± 1.9 %; S phase, 34.55 ± 0.98 %; and G2/M phase, 26.24 ± 1.7 % of cell arrest were observed. The results demonstrated the effectiveness of the proposed design for the development of corn starch-coated QT-NLs and their activity in breast cancer cell lines.

* Corresponding author.
** Corresponding author.
E-mail addresses: praveenpharmaco@gmail.com (P.K. Pasala), rsmrpal@gmail.com, drmr_pharma@vignan.ac.in (M. Rudrapal).

https://doi.org/10.1016/j.heliyon.2024.e37430
Received 21 May 2024; Received in revised form 2 September 2024; Accepted 3 September 2024
Available online 4 September 2024

1. Introduction

One of the prominent malignant tumors affecting women, with a frequency of 2.2 million as of 2020, is breast cancer, whose symptoms can include breast lumps, changes in the shape of the breast, fluid secretion from the nipple, patchiness of the skin in acute cases, swelling of lymph nodes, shortness of breath, and yellowish skin in chronic cases. Almost 5–10 % of breast cancer cases can be attributed to genetic predispositions, but the toll is due to lifestyle disorders, ionizing radiation, and hormone replacement therapy [1]. Many treatment approaches have been used, but the search for a reduction in drug-related adverse effects is ongoing. Therefore, natural compounds such as flavonoids, such as quercetin, apigenin etc. which have the potential to be complementary or alternative medicines, are gaining attention for their ability to treat breast cancer. Quercetin (QT) (Fig. 1) is a natural compound that has been proven to have toxic effects on various types of cancer cells and is available in olive oil, tomatoes, coffee, bracken ferns, lettuce, citrus fruits, red grapes, and tea [2–4]. The anti-inflammatory and antioxidant activities of QT act synergistically with its anticancer activity, thus making it a reliable option (Gibellini et al., 2011). The studies conducted by Ji and co-workers [5] on QT demonstrated its anticancer activity by suppressing the mobility of breast cancer cells through the glycolysis-mediated autophagy-induced Akt-mTOR pathway.

The problems with the delivery of QT lie in its low solubility and low permeability, which contribute to its low bioavailability; moreover, its polyphenolic nature limits the selection of delivery systems [6]. To address the hurdles offered by QT, liposomal technology can be used for the successful delivery of QT. Liposomes are hydrophobic and hydrophilic in nature and provide better stability to QT by binding the hydroxyl (OH) group of QT to its hydrophilic part. The hydrophobic part of liposomes helps to increase the permeability of the drug. The efficient delivery of drug molecules to the tumor site with minimal adverse effects associated with the drug is a major challenge in the treatment of cancer (Niazvand et al., 2019). To overcome these challenges, drug delivery systems have been investigated (Ezzati et al., 2020). Therefore, liposomes can enhance the delivery of QT via dual technology. In addition, liposomes are attractive options because of their easy formulation and wide range of possible modifications. In addition, they also have the benefit of scaling-up.

A vast variety of drug delivery approaches, such as micelles, solid lipid nanoparticles, polymeric nanoparticles, and liposomes have been studied for the delivery of QT [7]. Recently, many studies have focused on conjugating natural substances, such as bioflavonoids, with synthetic anticancer drugs, and drug delivery systems have been developed. One study focused on the simultaneous liposomal delivery of QT and vincristine to target breast cancer (Wong and Chiu 2010), and another similar study combined QT with mycophenolic acid to harness its chemotherapeutic activity in breast cancer [8]. Studies utilizing a combination of these two natural compounds are also available. One study combined QT and curcumin to design liposomes for cancer treatment [9]. Other studies have utilized the nanoparticle approach to harness the activity of QT in breast cancer [10].

Designing drug delivery nanosystems with minimal toxicity to both organisms and the environment remains a significant challenge. Ideally, nanocarriers should be swiftly cleared from the body after releasing their therapeutic payload. Lipid-based nanoparticles typically exceed the renal filtration threshold necessitating their opsonization by serum proteins and subsequent uptake by the mononuclear phagocyte system in organs such as the liver, kidneys, spleen, lungs, and lymph nodes for effective elimination. Although fenestrations in the spleen can filter out particles larger than 200 nm, the deformability of particles can enable larger ones to pass through and persist in the bloodstream. Toxicological outcomes are significantly influenced by the route of administration. For instance, when solid lipid nanoparticles (SLNs) and nanostructured lipid carriers (NLCs) are administered orally, they can undergo erosion and degradation due to the action of bile salts and pancreatic lipase. However, caution is necessary when handling cationic SLNs and NLCs due to potential *in vivo* toxicity. In a study [11] it has been reported that SLNs with different surface charges and polyethylene glycol (PEG) densities exhibited toxicity to platelets and, to a lesser extent, red blood cells. The study indicated that the toxic effects were influenced by the surface charge, with higher positive charges being more toxic, and by PEG density, with lower densities being more toxic [12]. Negatively charged liposomes, which are made of anionic lipids, have been found to be less stable compared to neutral or positively charged liposomes. Additionally, they are quickly absorbed by the reticuloendothelial system, which can result in toxic side effects [13]. Consequently, anionic liposomes are not commonly employed as drug carriers [14]. However, previous research has indicated that anionic, neutral, and cationic liposomes containing siRNA demonstrate low cytotoxicity, extended

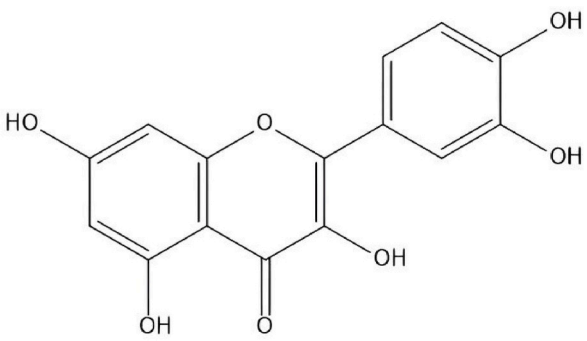

Fig. 1. Structure of quercetin.

circulation times, and efficient knockdown of target proteins in breast cancer cells [15]. However, distinct hazards are associated with various types of nanoparticles. For example, metal and metal oxide nanoparticles are mainly linked to DNA damage and the generation of reactive oxygen species. In contrast, polymeric nanoparticles have been observed to cause membrane leakage [16]. Polymeric nanodrugs can induce various toxic effects, including enhanced cytotoxicity, compromised cell viability, elevated rates of apoptosis (programmed cell death), potential for tumor initiation, DNA damage, gene toxicity, disruption of cell membranes, and lipid peroxidation reactions [17].

Several targeting external trigger techniques were developed earlier, but as a novelty of this in this work, the targeting agent corn starch was coated with a developed nanoliposomal formulation to enhance the delivery of QT to cancer cells. Hence, in the present study, we developed targeted QT nanoliposomal technology to enhance the safety and efficacy of the developed formulation for treating breast cancer. Most of the marketed forms available on the market are in the form of tablets and capsules, whereas the developed formulation is a lipid type with a targeting agent that can be easily taken up and is compatible with cells. As it contains natural phytoconstituents, the formulation is free from side effects, toxic effects, and biocompatibility, unlike synthetic drugs. Natural phytoconstituents present a promising alternative to synthetic drugs due to their superior biocompatibility, fewer side effects, and diverse therapeutic properties. These compounds are derived from plants and are generally well-tolerated by the body [18]. In our recent study, we developed nanoliposomes designed to target specific cancer cells, thereby enhancing targeting efficacy and minimizing side effects. Apart from that the phosphatidylcholine present in the formulation required for survival of cancer cells their uptake also results in higher drug concentration to the cancer cells there by effectively targeting cancer cells and reducing the side effects.

2. Materials and methods

2.1. Materials

Quercetin (QT) with 98 % purity was procured from TCI Chemicals, Hyderabad, India. Egg phosphatidylcholine (PC), cholesterol (CHOL), and cornstarch were purchased from Sigma-Aldrich, Bangalore, India. All the reagents used in this study were of analytical grade.

2.2. Method development by UV spectrophotometry

A standard stock solution was prepared by dissolving 100 mg of pure QT in 100 mL of phosphate buffer (PB) of pH 7.4, which corresponded to 1000 μg/mL. After the drug was completely dissolved, further dilutions were performed to obtain concentrations in the range of 10–200 μg/mL. Subsequently, the absorbance was determined using UV–visible spectrophotometer (Shimadzu) at a fixed wavelength of 375 nm. The buffer served as a blank and for adjusting the volume of the dilutions. The absorbance values were further used to plot the standard curve, and the regression value and standard curve equation were used [19].

2.3. Method development by HPLC

HPLC (Agilent) with a UV–visible detector and running on EZChrom Elite software [20,21] was utilized to analyze the samples and subsequent data collection and integration. The solvent (mobile phase) used was methanol:acetonitrile:aqueous orthophosphoric acid

Table 1
Experimental runs and observed responses for central composite design.

Std	Factor 1	Factor 2	Factor 3	Response 1	Response 2
	A: D:Lipid %	B: CHOL mg	C: ST min	VS nm	EE %
1	1.00	50.00	30.00	11.00	89.32
2	3.00	50.00	30.00	39.24	80.43
3	1.00	100.00	30.00	235.60	69.11
4	3.00	100.00	30.00	12.82	89.90
5	1.00	50.00	45.00	12.93	84.36
6	3.00	50.00	45.00	652.00	58.95
7	1.00	100.00	45.00	10.80	90.24
8	3.00	100.00	45.00	25.00	94.36
9	0.32	75.00	37.56	816.30	62.52
10	3.61	75.00	37.52	28.00	93.85
11	2.00	32.90	37.53	34.00	85.64
12	2.00	117.00	37.52	24.00	92.62
13	2.00	75.00	24.80	50.00	85.43
14	2.00	75.00	50.14	35.00	89.72
15	2.00	75.00	37.57	95.00	79.93
16	2.00	75.00	37.56	100.00	80.42

*D:Lipid% = Drug:Lipid; CHOL = Cholesterol; ST = Stirring time; VS = Vesicle size; EE% = % Entrapment efficiency.

(20:65:15). The flow rate was maintained at 1.0 mL/min, and the wavelength was 375 nm. A reversed-phase Ecosil C18 column (250 × 4.6 mm, 5 μm) at 25 °C was used for the study. The injection volume was 20 μl. The validation was performed for the developed method to assess various parameters, such as linearity, precession, interday precession, accuracy, and robustness as per International Council for Harmonisation of Technical Requirements for Pharmaceuticals for Human Use (ICH) guidelines. The linearity was determined by preparing six standard QT solutions with concentrations ranging from 5 to 30 μg/mL. The linear increase in the absorbance was determined to ensure that the linearity test was successful. The precision of the developed method was confirmed by repeatability and intermediate precision. Intraday precession analyses were performed by repeating the method three times on the same day and three successive days. The absorbance was determined, and the percentage RSD was calculated. Accuracy was calculated based on three different trials of the sample, each with a triplicate sequence for more reliable data. The system suitability parameters were assessed by standard solution injection and the flow rate robustness was assessed by increasing the flow rate from 0.8 to 1.0 mL/min [20,21].

2.4. Fourier transform infrared (FT-IR) spectroscopy

The drug was confirmed using a Bruker Alpha FT-IR spectrophotometer. The drug was subjected IR analysis by KBr pressed pellet method. The IR spectrum ranged from 400 to 4000 cm^{-1}. The same procedure was used for FT-IR analysis of the physical mixture.

2.5. Design of experiments (DoE)

The DoE approach was used to optimize QT-NLs after a critical review of the literature and few formulation trials [22,23]. A total of 16 QT-NL formulations were designed by central composite design (CCD) of Design Expert software version®13. The independent and dependent factors used in the study are listed in Table 1. The diagnostic plots, ANOVA, and contour plots were used to obtain the optimized formulation [5,24].

2.6. Preparation of QT-NLs

A fixed amount of 50 mg of QT was dissolved in 3 mL of ethanol. Tween 80 (1 %) was added into it to increase the solubility. To the resultant mixture of tween 80 and ethanol, PC and CHOL were added simultaneously with constant stirring until a clear dispersion was formed, indicating lipid phase formation (Step 1). They were then placed in a rotary vacuum evaporator, and the process was continued at 60 °C for 1 h to obtain a thin lipid film. The film was hydrated with phosphate buffered saline (PBS) of pH 7.4 and stirred for 30–50 min. The formed liposomes were added dropwise to the aqueous phase previously dissolved with corn starch under constant magnetic stirring (REMI 2MLH) in the range of 800–1000 rpm at 55 °C (Step 2). The stirring time varied from 37.5 to 45 min for the different formulations. The resultant formulation was subjected to probe sonication (Electrosonic Industries, MM1010) with a frequency of 20 kHz at a fixed temperature (37 °C) initially for 2 min followed by another 3 min with a gap interval of 15 s. The corn starch-coated QT-NLs were stored in suitable containers and used for various characterization studies.

2.7. Characterization

2.7.1. Determination of solubility characteristics of pure QT

A solubility study of the pure QT drug was carried out by the addition of an excess amount of the sample to 15 mL of distilled water under constant stirring in an orbital shaker. The solution was analyzed spectrophotometrically at 375 nm.

2.7.2. Vesicle size (VS) and polydispersity index (PDI)

The VS (Z-avg) and PDI of QT-NLs were determined by dynamic light scattering (DLS) using a zeta sizer (Horiba SZ-100 series) at 25 °C. The liposomal formulation of QT was diluted 100 times with analytical-grade water and subsequently analyzed. All runs were performed in triplicate.

2.7.3. Zeta potential (ZP)

The physical stability of the formulation was determined by the particle charge. The particle charge was quantified as the ZP. The electrophoretic mobility of particles in an electric field determines the ZP. The zeta potential of the formulations was determined using a HORIBA SCIENTIFIC SZ-100 ZETA SIZER instrument at 25 °C. For the zeta analysis, the sample was subjected to prior dilution (1:500) with distilled water. The measurements were performed in triplicate to ensure more reliable data [20].

2.7.4. FT-IR study

The compatibility of the pure drug and excipients was evaluated using FT-IR spectroscopy. This goal was achieved by overlapping and mapping the wave numbers of pure QT and the physical mixture of excipients. The obtained peaks were compared to ascertain the possibility of incompatibility.

2.7.5. Entrapment efficiency (EE)

The entrapment efficiency of the liposomal formulation was determined with the help of the developed HPLC method. Approximately 5 mL of the QT-NL formulation was mixed with another 5 mL of PB and centrifuged (14000–15000 RPM for 15 min). Subsequently, the supernatant was collected and diluted. The data obtained by analyzing the supernatant indicated an unentrapped

amount. The percentage EE (%EE) was calculated using the following formula:

% EE = (WT-WF) / WT X 100

where, WT = Total amount of the drug taken initially in the formulation, WF = Amount of the free drug present in the supernatant.

2.8. In vitro drug release study

The cumulative percentage of drug release was studied using a dialysis membrane. To make the membrane accustomed to usage, a fixed measurement of the membrane (length of 5.9 cm, width of 2.6 cm, and area of 15.34 cm^2) was dipped in a solution of 0.5 mL of glycerin and 50 mL of PB for 24 h. A 5 mg equivalent of the optimized QT-NL was placed in the dialysis membrane, and the setup was tied properly. The membrane containing the formulation was dipped in a beaker containing 200 mL of PB at 37 ± 1 °C. A constant magnetic stirring speed of 25 rpm was maintained. Samples were collected at predetermined intervals (1, 2, 4, 6, 8, 10, 12, 24, 48, 60, and 72 h).The collected samples were analyzed using the developed HPLC method [25].

2.9. Morphology measurement

Scanning electron microscopy (SEM) was used to determine the morphology of the resultant formulation. To do so, the QT-NLs were spread on a glass slide followed by vacuum air-induced drying, resulting in the formation of a thin film, which was subsequently subjected to SEM analysis. This analysis was performed at NISHKA LABS, Hyderabad, India.

2.10. MTT (3-(4,5-dimethylthiazol-2-yl)-2,5-diphenyltetrazolium bromide) assay (VERO and MCF-7 cell lines)

First, 200 μL of the cell suspension without the test substance was seeded in a 96-well plate such that the cell density was maintained at 20,000 cells per well. The cells were allowed to grow overnight. Next, the test agent at the appropriate concentration was added, and the plates were incubated for 24 h at 37 °C in a 5 % CO_2 environment. After the specified period of incubation, the plates were removed from the incubator, and MTT reagent was added to a total volume of 0.5 mg/mL. Then, the plates were wrapped in aluminum foil to avoid exposure to light and transferred to an incubator for 3 h. In the next step, the MTT reagent was removed, and 100 μL of DMSO, which acts as a solubilizer, was added. To enhance the dissolution, gentle stirring was performed in a gyratory shaker. In dense cultures, occasional pipetting up and down may also be required to aid in the dissolution of MTT formazan crystals. Subsequently, the absorbance at 570 nm and 630 nm was recorded using a spectrophotometer or ELISA reader [26,27]. Subsequently, the IC_{50} value was determined using linear regression, that is, $y = mx + c$, where $Y = 50$, and the values of M and C were derived from the viability graph. The study was outsourced from Stellixir Biotech Pvt. Ltd., Bangalore, India.

2.11. Propidium iodide apoptosis cell cycle assay

MCF-7 cells were cultured in 6-well plates at 2×10^5 cells/mL and incubated for 24 h at 37 °C in a CO_2 incubator. The spent medium was aspirated and washed with 1 mL of PBS (pH 7.4), followed by treatment with the optimized formulation at the desired concentration and incubation for 48 h. The cells were collected by trypsinization at the end of treatment and harvested into 5 mL vials. The mixture was then centrifuged (1800 rpm for 5 min). The cells were then washed with PBS and centrifuged again at 1800 rpm for 5 min. The cells were fixed with 1 mL of prechilled absolute ethanol at 4 °C for 1 h to permeabilize the cells. The mixture was centrifuged again under the above conditions, and excess ethanol was removed by washing with PBS and centrifuging. Finally, the cells were treated with 400 μl of propidium iodide staining buffer and mixed thoroughly. The samples were incubated for 15–20 min at room temperature in the dark and analyzed by flow cytometry.

2.12. Stability of nanoliposomes

The stability of the optimized nanoliposome was tested by maintaining it at 5 °C for three months. At the end of 90 days, samples were collected and examined for changes in vesicle size and drug content.

3. Results

3.1. Analytical studies

The analytical method for QT was performed using the UV–visible spectrophotometric method at 375 nm, and a standard graph was generated. It obeyed Beers-Lambert's law in the range of 10–200 μg/mL.

The analytical method developed by HPLC also reported satisfactory results, which were supported by the desired parameter values of precision, accuracy, robustness, linearity, and specificity at 375 nm (supplementary file, Fig. S1, Tables S1–S5). The injection volume used was 20 μl. After successful completion of the runtime, the area of the desired peak was recorded and this was subsequently used to quantify the amount of QT.

3.2. FT-IR study

The FT-IR spectroscopic study was performed to confirm the presence of QT. The characteristic peak frequencies corresponding to the functional groups are mapped and presented in Table 2 and Figs. S2 and S3 (supplementary file). In addition to the identification of QT, an FT-IR study of the physical mixture of QT and excipients was carried out, which served as a compatibility study on the pre-formulation criteria.

3.3. VS and PDI

The VS and PDI of QT-NLs were estimated using a Nano sizer (Horiba SZ-100). The vesicle size of the optimized formulation was 39.5 nm, with a PDI of 0.251 cm^2/vs (Fig. 2A).

3.4. ZP

The ZP was determined using a nanosorbent (Horiba SZ-100) to determine the physical stability of the NLs. The ZP of the optimized QT-NLs was found to be −41.2 mV (Fig. 2B).

3.5. Morphology measurement

The SEM analysis of the optimized formulation yielded satisfactory results, exhibiting an imperfect crystalline morphology.

3.6. In vitro drug release

The dissolution profile of QT-NLs showed 68.85 ± 2.4 % drug release by the end of 72 h (Fig. 3). QT-NLs showed sustained drug release. Owing to the reduction in vesicle size, QT-NL exhibited improved solubility and an increased dissolution rate. The zero-order, first-order, Higuchi, and Korsmeyer-Peppas plots were generated for QT-NL and are shown in Fig. 4A–E. The R^2 values of the first-order and Higuchi models were close to each other, but slightly greater than the value of the Higuchi model, suggesting that it followed the Higuchi model rather than the zero-order, first-order, Korsmeyer-Peppas, or Hixson-Crowell models.

3.7. Statistical analysis (ANOVA)

The reported model F values were 4.16 and 3.79 for VS and EE, respectively, which suggested that the model is significant, and a chance of only 0.31 % (VS) and 0.81 % (%EE) is there that this F value would have resulted from noise. The p value was also less than 0.0500, indicating that the model terms were significant. A, AB, AC, BC, and A^2 were significant terms reported for VS, whereas for EE, the reported significant terms were B, AB, and AC. Terms with a value greater than 0.1000 were considered insignificant. The coefficient estimate is a measure of the expected change that would arise in response to a one-unit change in factor. The overall average response for all runs is indicated by the intercept. The polynomial equation for the structures was derived from the respective estimates of the responses (Table 3).

3.8. Effect of statistically significant plots on responses

3.8.1. Box–Cox plot

The selection of the required power transformation to be applied to the response data was derived using the Box–Cox plot. Data transformations were characterized using a power function. Responses with a value greater than zero are susceptible to power-law transformation. The applied power transformation, minimum lambda values, and lambda values at a 95 % confidence range are displayed in the plot.

Table 2
FT-IR interpretation.

Pure quercetin		Physical mixture (Quercetin + Excipients)	
Spectra band	Functional group	Spectra band	Functional group
3226.88	Bonded OH (Intermolecular dimeric)	3302.67	Bonded OH (Intermolecular dimeric)
3486.67		3546.26	
1240.73	C-O stretching (cyclic ether)	1748.21	C=O stretching (ester)
1662.39	C=O stretching	2919.66	C–H stretching, CH_3
1168.42	C-O stretching	1439.99	C–H deformation, CH_3
1367.00	O-H deformation	1236.20	C-O stretching
		1387.48	O-H deformation
		2851.86	C-H stretching in (N-CH_3)

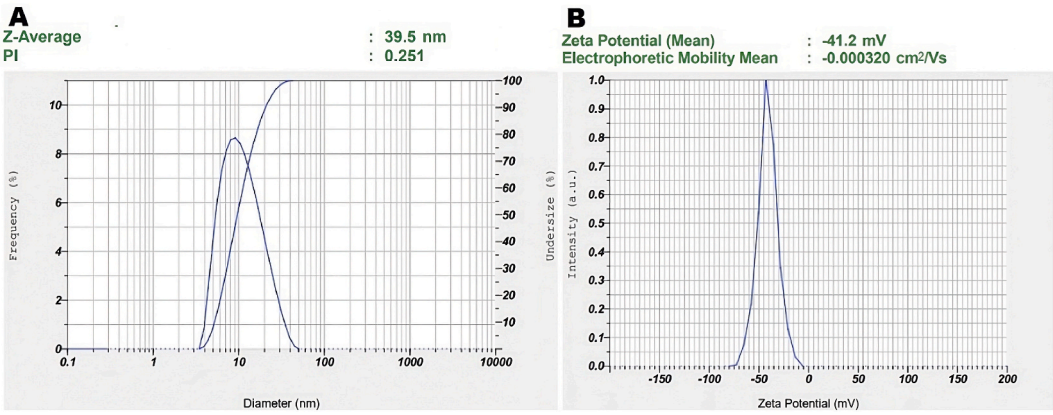

Fig. 2. Typical graph representing (A) VS and PDI and (B) ZP of QT-NL formulation.

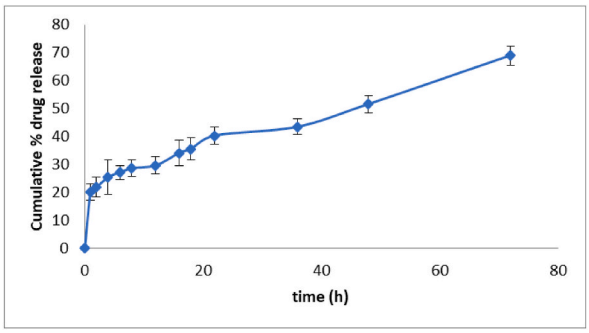

Fig. 3. %Cumulative drug release of QT from QT-NLs optimized formulation (mean ± SD, n = 3).

3.8.2. Predicted vs. actual plot

The predicted and actual values were close in both cases, which is indicative of their suitability.

3.8.3. Residuals vs. predicted plot

A plot between the ascending predicted response and residuals can be used to test the assumptions of constant variance. The random scattering of the data points, contrary to the megaphone pattern, indicates that no such transformation is needed.

3.8.4. Normal plot vs. residual plot

This plot is used to indicate the normal distribution of residuals along a straight line. The miniature S-shaped distribution of the data points indicates the need for transformation.

3.8.5. Cook's distance plot

This plot indicates the amount of change that would be incorporated in the entire regression function if the point under consideration is not included for model fitting; that is, it denotes the summation of the difference in prediction caused by not considering the specific point for analysis.

3.8.6. Leverage vs. run plot

This plot shows the degree of influence that a point can have on the model fit. A leverage of 1 indicates that the model fits exactly at that point, and if the point is more than twice the average, then it is said to have high leverage over the model. In the diagnosis of vesicle size, it was observed that all the data points were nearby, and no such leverage point was detected, which indicated that all the data points had almost similar leverage. However, for entrapment, it was observed that the points divided themselves at almost a certain value, which is indicative of the presence of leverage.

3.8.7. Interaction plot

Contrary to the perturbation plot, this graph provides an idea of the combinational interaction of the factors on the response. The intersecting lines of the graph are evident because a significant level of interaction was present. This plot helps to compare the effects of all factors in a one-factor-at-a-time manner.

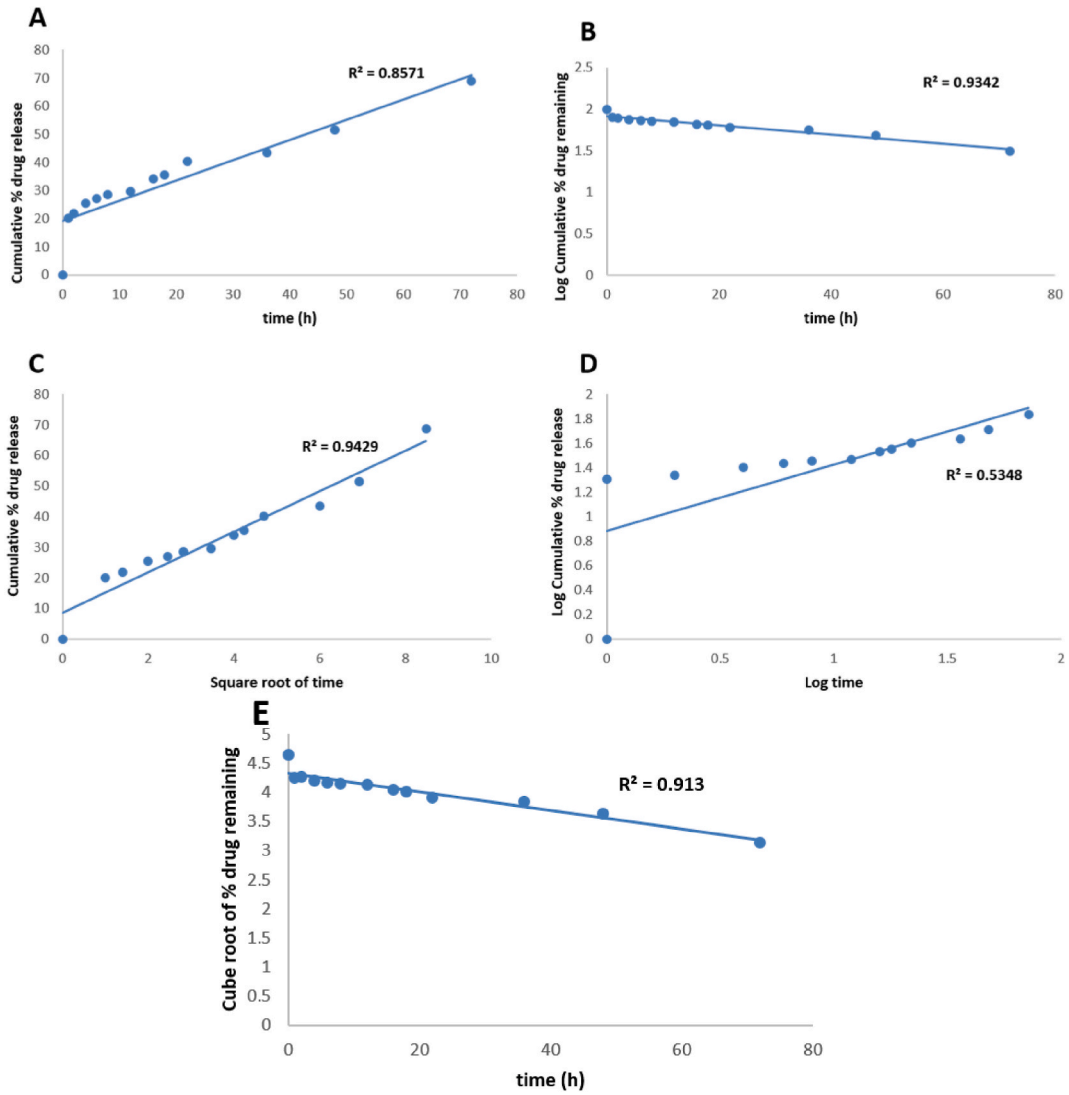

Fig. 4. Drug release kinetics of QT-NLs. (A) Zero order, (B) First order, (C) Higuchi, (D) Korsmeyer-Peppas plot, (E) Hixson-Crowell plot.

3.8.8. Perturbation plot

This plot helps to compare the effects of all factors in a one-factor-at-a-time manner. This approach does not provide any description of the interaction between these two parameters. The steep slopes of Factors A and B indicated sensitivity to vesicle size. On the other hand, the almost straight curve of Factor C is a marker of the insensitivity of the factor.

3.9. Effect of formulation variables on response Y1 (VS)

The model had an F value of 4.16, indicating that the model was significant. The probability of obtaining such an F value was 0.3 %, and the values of prob > F were less than 0.05, indicating that the model was significant. In this model, the terms A, B, C, AB, AC, BC, and A^2 are significant. The model terms were not significant if the values were greater than 0.05. When numerous insignificant model terms are present, model reduction is required to improve the model. In the present study, many model terms were less than 0.05, indicating that VS was more influenced by factor A than by factor B or factor C. A nonsignificant lack of fit was required to obtain an acceptable model. The adequate precision measure was 6.3144 (any value greater than 4 is acceptable); hence, this model can be used to navigate the design space [28]. The polynomial equation obtained for this model is as follows:

$$VS = 75.36–67.67A – 29.56B + 23.49C–102.43AB + 98.54AC – 97.38BCE + 112.19A^2– 026.02B^2 – 21.59C^2$$

Table 3
ANOVA for VS and %EE.

VS						
Source	Sum of squares	df	Mean Square	F value	p value	
Model	1.04E+06	9	1.16E+05	4.16	0.00	Significant
A-D:lipid	1.25E+05	1	1.25E+05	4.46	0.04	
B-CHOL	23867.99	1	23867.99	0.85	0.03	
C-ST	15068.48	1	15068.48	0.53	0.04	
AB	1.67E+05	1	1679E+05	5.99	0.02	
AC	1.55E+05	1	1.55E+05	5.55	0.02	
BC	1.51E+05	1	1.51E+05	5.42	0.02	
A^2	2.33E+05	1	2.33E+05	8.32	0.00	
B^2	12541.57	1	12541.57	0.44	0.51	
C^2	8635.61	1	8635.61	0.30	0.58	
Residual	6.16E+05	22	28017.75			
Lack of Fit	6.07E+05	5	1.21E+05	3.74	0.7964	Not Significant
Pure Error	8623.99	17	507.29			
Cor Total	1.66E+06	31				
%EE						
Source	Sum of squares	df	Mean Square	F-value	p value	
Model	1555.13	6	259.19	3.79	0.00	Significant
A-D:lipid	87.28	1	87.28	1.28	0.02	
B-CHOL	353.87	1	353.87	5.17	0.03	
C-ST	81.93	1	81.93	1.20	0.08	
AB	415.14	1	415.14	6.07	0.02	
AC	332.15	1	332.15	4.85	0.03	
BC	284.77	1	284.77	4.16	0.05	
Residual	1710.80	25	68.43			
Lack of Fit	556.69	8	69.59	1.03	0.45	Not Significant
Pure error	1154.11	17	67.89			
Cor Total	3265.93	31				

VS: Vesicle size, EE: Entrapment efficiency.

3.10. Effect of formulation variable on response Y2 (PDI)

The model was considered significant when the F value was 3.79. The model terms B, AB, AC, and BC were less than 0.05 and hence significant. The lack of a fit F value of 1.03 is not significant relative to the pure error. The adequate precision measure was 6.6745. The polynomial equation for this model is as follows.

$$\%EE = 83.69 + 1.79A + 3.60B + 1.73C + 5.09AB - 4.56AC + 4.22BCE$$

The contour plots, 3D surface plots, and overlay plots are depicted in Fig. 5A–E.

3.11. Optimization

The optimized formula was selected after careful analysis of the design space and setting up the constraints and overlay plot study (Table 4).

3.12. MTT assay

3.12.1. VERO cell line

After 72 h, VERO cells treated with the developed QT-NL formulation at 75 and 150 μg/mL exhibited 97.89 % and 77.64 % cell viability, respectively. Fig. 6A shows untreated cells that were free from apoptosis and were healthy; Fig. 6B and C represent the uptake of QT nanoliposomes at 75 and 150 μg/mL, respectively, with a CC_{50} value of 102 μg/mL, indicating the viability of cells at that concentration when observed under an inverted microscope. At 150 μg/mL, the normal morphology of the cells was disrupted. Furthermore, at 300 μg/mL, the number of treated cells decreased, and the cells were rounded with necrotic or apoptotic bodies, with distorted shapes and shrinkage, followed by membrane bleb formation and cytoplasmic condensation (Fig. 6D). The CC_{50} value of 102 μg/mL on VERO cells indicates the safety of the developed nanoliposomal formulation, as it was greater than 100 μg/mL; that is, it is safer to use in humans without any cytotoxicity.

3.12.2. MCF-7 cells (efficacy)

The IC_{50} values formed the basis for comparing the inhibitory effects of pure QT and the liposomal formulation of QT on the growth of MCF-7 cells. A total time frame of 72 h was used to obtain the exposure data required for the computation of IC_{50} values. The observed IC_{50} values for QT-NL were significantly lower than those for pure QT, at 5.8 μM and 7.9 μM, respectively. The data obtained

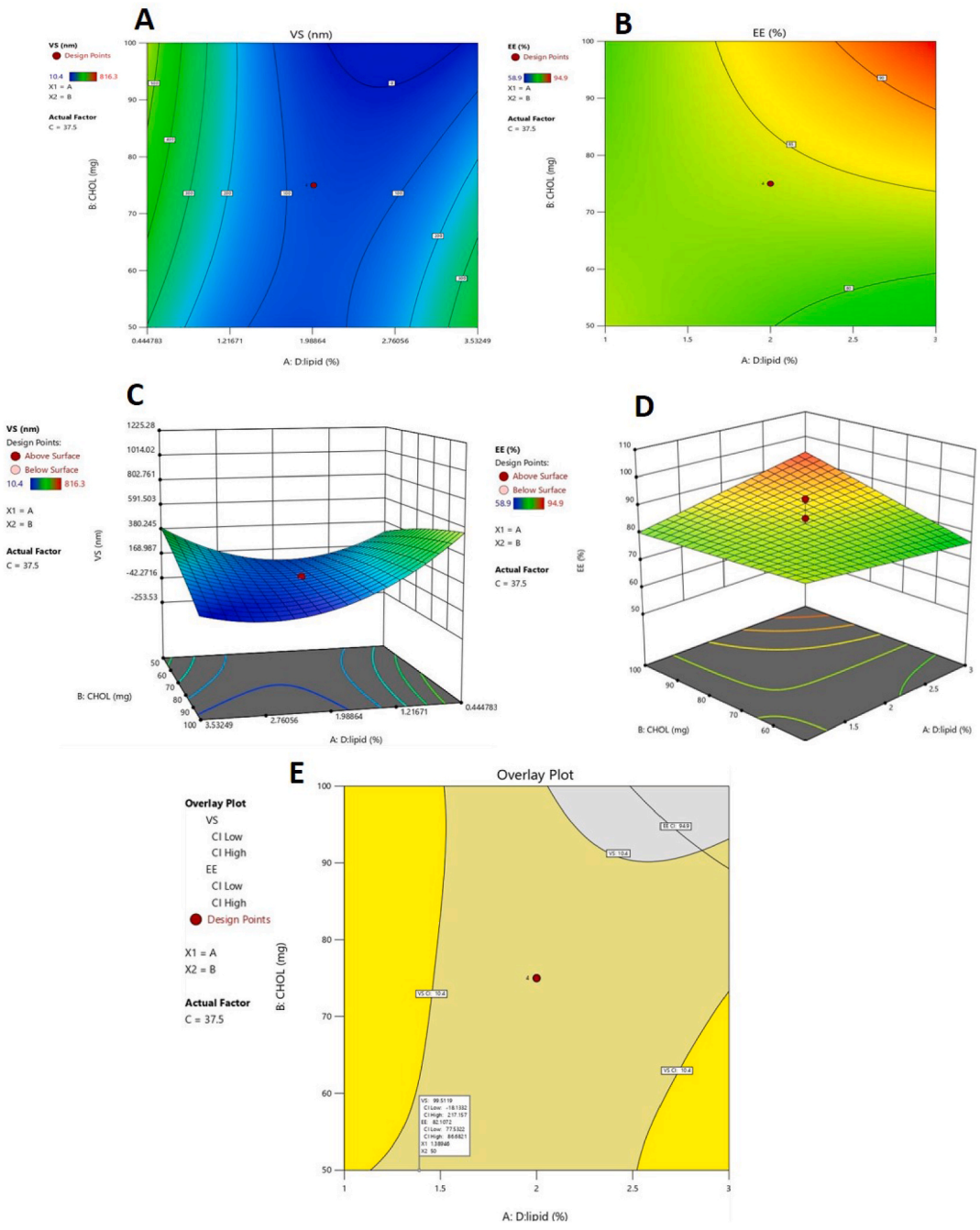

Fig. 5. Contour plot of QT−NL formulation. (A) VS, (B) EE, (C) 3D response surface plot of VS, (D) EE, (E) Overlay plot. VS: Vesicle size, EE: Entrapment efficiency.

confirmed that QT-NL was undoubtedly better at reducing cell viability than pure QT or the standard (12.5 μM quinacrine). A plot of % cell viability in relation to drug concentration was plotted to provide an overview (Fig. 7 A and 7B).

3.13. Cell cycle arrest of MCF-7 cells (propidium iodide apoptosis assay) induced by targeted QT-NLs

Khorsandi and co-authors [29] demonstrated that compared to the control and free QT, the developed solid lipid nanoparticles significantly increased the percentage of late and early apoptosis and necrosis in MCF-7 cells. No effect was observed on the blank formulation when treated with MCF-7 cells. In our study, the optimized formulation exhibited late and early apoptosis and necrosis when used to treat MCF-7 cells. The S and G2/M cell cycle phase of MCF-7 cell arrest confirmed by the cell cycle report. At sub-G0/G1

Table 4
Constraints data.

Name	Goal	Lower limit	Upper limit	Lower weight	Upper weight	Importance
A: Drug:Lipid	Is in range	1	3	1	1	5
B: CHOL (mg)	Minimize	50	100	1	1	3
C: Stirring time (min)	Is target = 37.5	30	45	1	1	4
VS (nm)	Minimize	10.4	816.3	1	1	5
EE (%)	Maximize	58.9	94.9	1	1	3

CHOL: Cholesterol, VS: Vesicle size, EE: Entrapment efficiency.

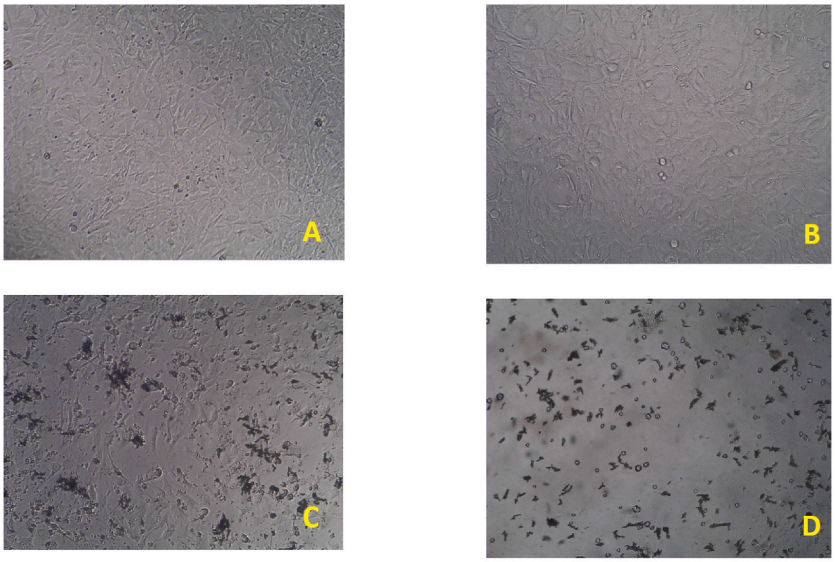

Fig. 6. Morphology of VERO cell line after treatment with QT-NL formulation after 72 h treatment. (A) Untreated cells, (B) QT-NL formulation at 75 μg/mL, (C) QT-NL formulation at 150 μg/mL, (D) QT-NL formulation at 300 μg/mL.

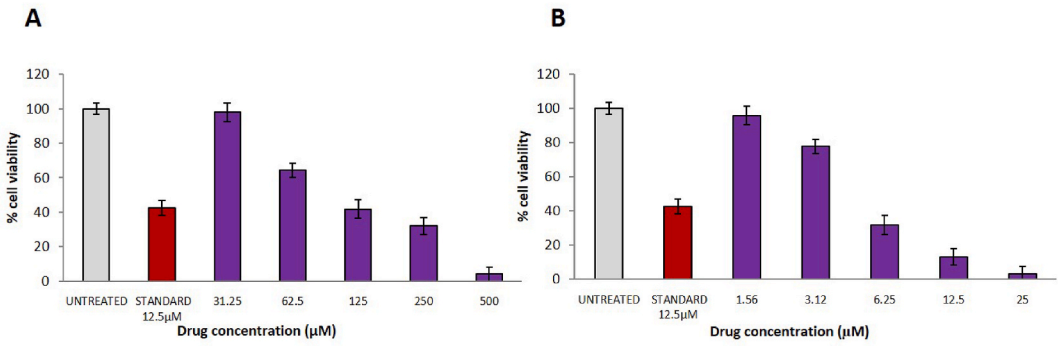

Fig. 7. MTT assay of MCF-7 cells treated with (A) pure QT and (B) QT-NL (mean ± SEM, n = 3).

phase, 2.10 ± 1.1 %; G0/G1 phase, 34.13 ± 1.9 %; S phase, 34.55 ± 0.98 %; and G2/M phase, 26.24 ± 1.7 % cell arrest was observed (Fig. 8).

3.14. Stability analysis

The optimized formulation was inspected for VS and drug content after the stipulated period, as per ICH guidelines, for 6 months. The data obtained provided evidence of the stability of the formulation under the tested conditions.

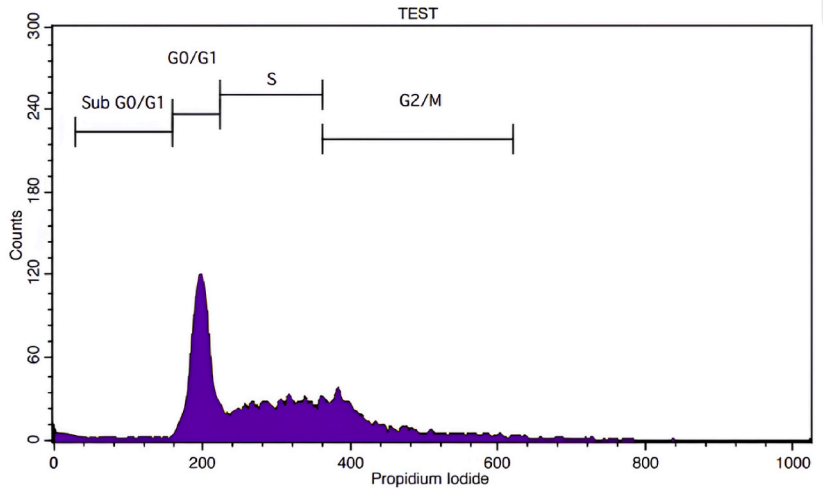

Fig. 8. Flow cytometric histograms showing the phases of cell cycle distribution on MCF-7 cell line treated with optimized QT-NLs at 5.8 μM concentration.

4. Discussion

The R^2 value obtained by plotting the absorbance versus concentration was 0.9992, indicating that the calibration curve was linear and confirming the effectiveness of the developed method. From HPLC analytical studies, the R^2 value of 0.9987 indicates that the developed method was well calibrated and yielded linear results. The %RSD was also calculated for all the parameters of the test. The accuracy results revealed that at each level, the average recovery was between 98.86 %, 99.29 %, and 99.39 %, with an RSD $\leq$1 %, which confirmed the accuracy of the method. The FT-IR studies indicated that there was a shift of a few peaks in the physical mixture compared to the pure drug, which indicated the formation of bonds. The physical mixture also exhibited new peaks, which are characteristic of bond formation between the drug and the excipients. This indicates that the hydroxy group of cholesterol engaged with the carbonyl group of phospholipids, potentially augmenting the hydration around the lipid head groups by expanding the inter head group distance. In a physical mixture heightened CHOL integration correlates with an elevated occurrence of the C=O stretching band, indicative of liberated carbonyl groups within the system was observed [30].

The ethanol injection and reverse-phase evaporation technique was adopted for the formation of liposomes. This method has unique advantages in that controlled uniform-sized vesicles with increased encapsulation can be achieved; additionally, lipid bilayer destabilization and liposome formation can be achieved in the presence of ethanol. The careful optimization of several parameters, such as lipid concentration and composition, hydration medium, temperature and time, aids in the effective formation of liposomes with higher %EE. By maintaining the temperature at 60 °C and adding CHOL to provide enhanced loading of QT, the results were consistent with those of previous studies [23]. The determination of the partition coefficient of the PC component serves as a valuable metric for elucidating the dynamics of QT loading within liposomal structures. Remarkably, the logarithm of the partition coefficient (logP) of PC is approximately equal to that of CHOL, i.e., 7.68. The logP of the QT interval is approximately 1.77 (https://comptox.epa.gov/dashboard/) [23]. Studies have demonstrated that CHOL does not impact the membrane partitioning of QT in liquid-disordered membranes, whereas it can enhance the accumulation of QT in CHOL-enriched, ordered membranes. It is hypothesized that cholesterol facilitates the establishment of membrane domains that enable the communication of QT across the lipid bilayer [31].

In the present study, the nanoliposomes were developed by designing an experiment-based central composite design approach rather than trial- and error-based methods. This approach offers unique advantages, as this approach offers an optimal solution amidst competing variables, requiring fewer experimental trials to attain the optimal formulation. This approach leads to considerable time and material savings, simplifies troubleshooting and rectification processes, and enables the estimation of interactions. Moreover, it facilitates the simulation of product or process performance using model equations and aids in seamless scalability. Based on a few formulation trials, it was observed that the drug:PC ratio, cholesterol content and stirring time affected nanoliposome formation. The interaction of cholesterol and PC in liposomal formulations reduced the particle size distribution, suggesting that cholesterol could impede interparticulate interactions that typically result in increased particle size. The presence of unpacked hydrophobic domains within the membrane, attributed to unsaturated tails, might facilitate interparticle interactions. It is plausible that cholesterol tends to inhibit such hydrophobic interactions among liposomes [23].

Further mechanical stirring might have resulted in the breaking of agglomerates, and the generated shear forces and surface energetics reduced the cohesive forces of the particles, resulting in a uniform distribution. Maintaining the ratio of drug:PC (1:3) and CHOL (50 mg) and stirring for 37 min led to an effective %EE. An increase in cholesterol content resulted in a decrease in %EE. Earlier studies also reported that liposomes formulated with egg PC exhibited a %EE of 29.5 % for ibuprofen. However, with the addition of 30 % cholesterol, the EE decreased to 23.2 % and further decreased to 17.1 % with the addition of 50 % CHOL. Similarly, the

incorporation of cholesterol into vesicles resulted in reduced entrapment of lipid-soluble drugs. For instance, in the development of a cremophor-EL-free liposomal paclitaxel formulation, dioleoylphosphatidylcholine liposomes, an increase in CHOL content from 5 to 37 mol% led to a drastic decrease in %EE efficiency from 99.3 % to 6.2 %, respectively. However, there are instances where increasing the cholesterol content exhibited an opposite trend in terms of drug loading. Bhatia et al. reported that the addition of 30 % cholesterol increased the %EE of tamoxifen in PC liposomes from 45.2 % to 57.5 % [30,32–34]. These differences in the effects of CHOL on the % EE of hydrophobic compounds can be ascribed to individual molecular interactions among phospholipids, drug molecules and CHOL. The observation that CHOL enhances the hydrophobic nature within the central segment of the lipid bilayer may promote the incorporation of hydrophobic compounds. Conversely, considering that both cholesterol and the drug exhibit a preference for positioning themselves within the hydrophobic portion of the lipid bilayer and that there exists a finite space available for both cholesterol and hydrophobic drug molecules may compete for this spatial occupancy between the acyl chains of phospholipids, leading to diminished EE with increasing cholesterol content [30,35].

The morphology studies proved that the VS range was less than 100 nm, which satisfied the US Food and Drug Administration (FDA) particle size criteria. The PDI value was less than 1, which confirmed the uniform vesicle size distribution in the NLs [36]. The ZP confirmed the good stability of the NL. SEM analysis indicated that the nanoliposomes were formed successfully without any unwanted agglomeration, and no leakage was observed.

The *in vitro* drug release result can be described by the Noyes-Whitney equation (dx/dt = DA (Cs-Cty/hD)), where the proportionality of the saturation solubility (Cs) and dissolution rate (de/dt) led to better dissolution of NL. The overall improvement in the release of QT can be attributed to the enhanced permeability of QT due to the liposomal approach. The presence of PC and cholesterol in the formulation further enhanced the fluidity of the membrane in the nanoliposomes, which acted synergistically to provide an improved and sustained release profile [37]. The hydroxyl moiety within this structurally rigid segment of CHOL resides proximate to the ester carbonyl group, suggesting the presence of hydrogen bonding between these functional groups. Moreover, the steroid ring and the hydrophobic tail orient themselves within the upper hydrophobic region of the membrane, aligning parallel to the acyl chain of the phospholipid [30,38], and it could position itself near the membrane's glycerol backbone, restricting the movement of QT to the inner core. This phenomenon may explain the sustained release rates of QT.

According to the regression equation of vesicle size, A, B, and C indicate effects on vesicle size; AB, AC, BC, A^2, B^2, and C^2 are interactive terms that indicate a nonlinear relationship between the responses. A positive sign in the equation represents synergistic effects, and a negative sign denotes an antagonistic effect on VS [28]. This equation states that out of three variables, sonication time (C) has a positive effect on vesicle size, whereas the drug:lipid ratio (A) and CHOL concentration (B) have a negative effect on VS. In the present study, based on contour plots, 3D surface plots, and overlay plots [28], it was determined that stirring time had a significant effect on vesicle size, and increasing stirring time resulted in reduced VS and vice versa. The interaction terms AC and A^2 had positive effects on the response, whereas the other interaction terms had negative impacts on the response.

In the %EE regression equation, a positive sign represents synergistic effects, and a negative sign denotes antagonistic effects [28]. This equation shows that the drug:lipid ratio (A), CHOL concentration (B), and stirring time (C) had positive effects on the EE. The contour, 3D and overlay plots showed that the increases in A, B, C, and EE also increased. The incorporation of CHOL in liposomes up to 50 mg increased the efficiency of the vesicles and helped the liposomes entrap a larger amount of drug inside them. The interaction term AB and BC had a positive effect, whereas AC had a negative effect on the response. The optimized formulation was selected based on vesicle size and % EE.

The optimized NL was selected based on the desirability and feasibility of the experiment. The composition of the formulation was 1:3, 50.00 mg, and 37.50 min for the considered input variables-the drug:lipid ratio (A), cholesterol concentration (B), and sonication time (C), respectively. For the above variables, the predicted dependent variables were found to be (VS: 29.501 nm and %EE: 82.101) against the actual observed values (VS: 31.62 nm and %EE: 80.71). Subsequently, the % error was calculated, which was found to be 7.115 % and 1.706 % for the VS and EE, respectively, against the limit of ±10 %.

The enhanced efficacy of the QT-NL formulation toward tumor cells might be due to its enhanced permeability and retention effect that crosses over the neovasculature of tumor cells, which is discontinuous and leads to passive and retained accumulation. The endothelial tight intracellular junctions in normal cells may have restricted the permeation of QT-NL [39–41]. Apart from this, healthy cells might have utilized less corn starch; hence, the presence of the drug would be less than that of cancer cells and hence less toxicity toward healthy cells. The other reason is the presence of flavonoids in QT, which exhibit an apoptotic mechanism, thereby killing cancer cells without affecting healthy cells [42,43]. Several studies [44,45] have shown that phospholipids provide targeted delivery to cancer cells, i.e., cancer cells require more phospholipids for their regulation and metabolism than healthy cells. This might be another probable reason for the effective reduction in cancer cells after treatment with the developed QT-NL formulation. Compared to QT, the nanoliposomal form of QT, that is, its lipophilic property, enhances the permeability and intracellular uptake of the drug by passive targeting, thereby enhancing the efficacy of QT in treating breast cancer. This would also reduce systemic side effects and enhance overall therapeutic benefits [46,47].

The optimized formulation exhibited late and early apoptosis and necrosis in MCF-7 cells, possibly due to the effective uptake of the developed liposomal formulation, that is, the presence of phospholipids (lipophilic nature). Another reason might be the presence of corn starch and its enhanced intracellular uptake only by cancer cells, thereby providing maximum availability of the drug to particular cancer cells and enhancing apoptosis. This resulted in a reduction in the viability of the MCF-7 cells. Cell survival and apoptosis are often used as markers to verify the efficacy of anticancer agents. Furthermore, phosphotidyl choline assists in apoptosis [45]. Sun et al. provided similar results by proving the enhanced efficacy of the developed QT nanostructured lipid carriers on MCF-7 cells [48,49] by developing a self-nanoemulsifying delivery system and showing that it induced DNA damage and apoptosis in MCF-7 cells. Overall, increased apoptosis and reduced viability of MCF-7 cells were observed after treatment with the QT-NL formulation.

5. Conclusion

In comparison to other delivery systems, the ability of liposomal technology to address the hurdles offered by quercetin is remarkable and can be relied upon for the successful delivery of quercetin. Liposomes are hydrophobic and hydrophilic in nature and provide better stability to quercetin by binding the hydroxy group of quercetin to its hydrophilic part, and the hydrophobic part of liposomes helps to increase the permeability of the drug. In addition, the size range offered by the liposomes proved to be an additional advantage. Therefore, enhancing the delivery of quercetin via dual-technology corn starch-dispersed quercetin nanoliposomes further enhanced the activity. In addition, liposomes are attractive options because of their easy formulation and wide range of possible modifications. In addition, they also have the benefit of scaling-up. The application of DoE in the development process has made the product cost-effective, and DoE can be used as an adjuvant therapy with other drugs/formulations. The resistance of the product also decreased due to specific targeting and enhanced permeability, as the formulation was finally coated with corn starch. The safety and efficacy of quercetin were improved by its development into a nanoliposomal formulation, which was confirmed by enhanced apoptosis and reduced cell viability.

Data availability statement

The data are included in the manuscript and supplementary materials of this article.

Funding

This research was funded by King Saud University, Riyadh, Saudi Arabia, Project Number (RSPD2024R709).

CRediT authorship contribution statement

E. Bhargav: Project administration, Methodology, Investigation, Data curation. **Nawaz Mohammed:** Visualization, Software, Resources, Methodology, Investigation. **Udit Narayan Singh:** Validation, Supervision, Software, Project administration, Methodology. **P. Ramalingam:** Visualization, Validation, Software, Resources, Project administration, Investigation. **Ranadheer Reddy Challa:** Visualization, Validation, Investigation, Funding acquisition, Formal analysis. **Bhaskar Vallamkonda:** Writing – original draft, Visualization, Validation, Software. **Sheikh F. Ahmad:** Resources, Project administration, Methodology, Investigation, Funding acquisition. **Prasanth DSNBK:** Writing – original draft, Visualization, Validation, Software, Project administration, Methodology. **Praveen Kumar Pasala:** Writing – review & editing, Visualization, Validation, Supervision, Methodology, Investigation, Data curation. **Mithun Rudrapal:** Writing – review & editing, Writing – original draft, Validation, Methodology.

Declaration of competing interest

The authors declare that they have no known competing financial interests or personal relationships that could have appeared to influence the work reported in this paper.

Acknowledgments

The authors acknowledge and extend their appreciation to the Researchers Supporting Project Number (RSPD2024R709), King Saud University, Riyadh, Saudi Arabia, for funding this work. The authors are also thankful to DST-FIST Lab, Raghavendra Institute of Pharmaceutical Education & Research, Anantapur, India, for providing instrumentation support to carry out research.

Appendix A. Supplementary data

Supplementary data to this article can be found online at https://doi.org/10.1016/j.heliyon.2024.e37430.

References

[1] D. Das, Breast cancer: risk factors and prevention strategies, World J Biol Pharm Health Sci. 12 (3) (2022) 265–280.
[2] M. Rudrapal, S.J. Khairnar, J. Khan, et al., Dietary polyphenols and their role in oxidative stress-induced human diseases: insights into protective effects, antioxidant potentials and mechanism (s) of action, Front. Pharmacol. 13 (2022) 806470.
[3] M. Rudrapal, S. Maji, S.K. Prajapati, et al., Protective effects of diets rich in polyphenols in cigarette smoke (CS)-induced oxidative damages and associated health implications, Antioxidants 11 (7) (2022) 1217.
[4] M. Rudrapal, D. Chetia, Plant flavonoids as potential source of future antimalarial leads, Sys. Rev. Pharm. 8 (1) (2017) 13–18.
[5] L. Jia, S. Huang, X. Yin, et al., Quercetin suppresses the mobility of breast cancer by suppressing glycolysis through Akt-mTOR pathway mediated autophagy induction, Life Sci. 208 (2018) 123–130.
[6] M. Rudrapal, A.K. Mishra, L. Rani, et al., Nanodelivery of dietary polyphenols for therapeutic applications, Molecules 27 (24) (2022) 8706.
[7] M. Rudrapal, S. Vallinayagam, J.H. Zothantluanga, et al., Nanophytomedicines: nature to medicines, in: Applications of Nanotechnology in Drug Discovery and Delivery, Elsevier, 2022, pp. 71–93.

[8] G. Patel, N.S. Thakur, V. Kushwah, et al., Liposomal delivery of mycophenolic acid with quercetin for improved breast cancer therapy in SD rats, Front. Bioeng. Biotechnol. 8 (2020) 631.
[9] V. Ravichandiran, K. Masilamani, B. Senthilnathan, et al., Quercetin-decorated curcumin liposome design for cancer therapy: in-vitro and in-vivo studies, Curr. Drug Deliv. 14 (2017) 1053–1059.
[10] M. Gadhwal, S. Patil, P. D'Mello, et al., Synthesis, characterization and antitumour activity of some Quercetin analogs, Indian J Pharm Sci 75 (2013) 233.
[11] M.Y. Wong, G.N. Chiu, Simultaneous liposomal delivery of quercetin and vincristine for enhanced estrogen-receptor-negative breast cancer treatment, Anti Cancer Drugs 21 (2010) 401–410.
[12] Montoto S. Scioli, G. Muraca, M.E. Ruiz, Solid lipid nanoparticles for drug delivery: pharmacological and biopharmaceutical aspects, Front. Mol. Biosci. 7 (2020) 587997.
[13] H. Kiwada, H. Matsuo, H. Harashima, Identification of proteins mediating clearance of liposomes using a liver perfusion system, Adv. Drug Deliv. Rev. 32 (1998) 61–79.
[14] G. Bozzuto, A. Molinari, Liposomes as nanomedical devices, Int. J. Nanomed. 10 (2015) 975–999.
[15] J. Zhang, X. Li, L. Huang, Non-viral nanocarriers for siRNA delivery in breast cancer, J. Contr. Release 190 (2014) 440–450.
[16] V. Nadine, H. Petra, K. Sarah, et al., Toxicity of polymeric nanoparticles in vivo and in vitro, J. Nano Res. 16 (2014) 2379.
[17] S. Ananda Babu, A. Sanmugam, P. Ashwini, et al., Toxicity of polymeric nanodrugs as drug carriers, ACS Chem Health Saf 30 (2013) 236–250.
[18] M. Rudrapal, G. Rakshit, R.P. Singh, et al., Dietary polyphenols: review on chemistry/sources, bioavailability/metabolism, antioxidant effects, and their role in disease management, Antioxidants 13 (4) (2024) 429.
[19] A. Asfaram, M. Ghaedi, H. Javadian, et al., Cu-and S-@ SnO2 nanoparticles loaded on activated carbon for efficient ultrasound assisted dispersive μSPE-spectrophotometric detection of Quercetin in Nasturtium officinale extract and fruit juice samples: CCD-RSM design, Ultrason. Sonochem. 47 (2018) 1–9.
[20] E. Bhargav, G. Chaithanya Barghav, Y. Padmanabha Reddy, et al., A Design of Experiment (DoE) based approach for development and optimization of nanosuspensions of telmisartan, a BCS class II antihypertensive drug, Future J Pharm Sci 6 (2020) 1–13.
[21] E. Bhargav, Y.P. Reddy, K.B. Koteshwara, Development and optimization of luliconazole nanostructured lipid carriers based gel by quality by design its skin distribution studies, dermatokinetic modeling & in-vitro and ex-vivo correlation, Curr. Drug Deliv. 18 (2021) 1041–1053.
[22] J. Cristiano Ceron, N. Rezende, S. Daniela Fernandes, et al., Target selectivity of cholesterol-phosphatidylcholineliposome loaded with phthalocyanine for breastcancer diagnosis and treatment by photodynamictherapy, Photodiagnosis Photodyn. Ther. 39 (2022) 102992.
[23] H. Farzaneh, M. Ebrahimi Nik, M. Mashreghi, et al., A study on the role of cholesterol and phosphatidylcholine in various features of liposomal doxorubicin: from liposomal preparation to therapy, Int. J. Pharm. 551 (1–2) (2018) 300–308.
[24] T. Toniazzo, M.S. Peres, A.P. Ramos, et al., Encapsulation of Quercetin in liposomes by ethanol injection and physicochemical characterization of dispersions and lyophilized vesicles, Food Biosci. 19 (2017) 17–25.
[25] N. Najjari, S. Sari, M. Saffari, et al., Formulation optimization and characterization of Pistacia atlantica Desf. essential oil-loaded nanostructured lipid carriers on the proliferation of human breast cancer cell line SKBR3 (in vitro studies), J. Herb. Med. 36 (2022) 100600.
[26] L. Khorsandi, M. Orazizadeh, F. Niazvand, et al., Quercetin induces apoptosis and necroptosis in MCF-7 breast cancer cells, Bratisl. Lek. Listy 118 (2017) 123–128.
[27] F. Rezaie, M.J. Mokhtari, M. Kalani, Quercetin arrests in G2 phase, upregulates INXS LncRNA and downregulates UCA1 LncRNA in MCF-7 cells, Int J Mol Cell Med 10 (2021) 208–216.
[28] N. Sathyamoorthy, D. Magharla, P. Chintamaneni, et al., Optimization of paclitaxel loaded poly (ε-caprolactone) nanoparticles using Box Behnken design, Beni-Suef Univ J Basic Appl Sci 6 (2017) 362–373.
[29] L. Khorsandi, M. Orazizadeh, F. Niazvand, et al., Quercetin induces apoptosis and necroptosis in MCF-7 breast cancer cells, Bratisl. Lek. Listy 118 (2017) 123–128.
[30] D. Asli, S. Asli, S. Feride, et al., Celecoxib-loaded liposomes: effect of cholesterol on encapsulation and in vitro release characteristics, Biosci. Rep. 30 (2010) 365–373, 2010.
[31] A.C. Alves, A. Magarkar, M. Horta, et al., Influence of doxorubicin on model cell membrane properties: insights from *in vitro* and *in silico* studies, Sci. Rep. 7 (2017) 6343.
[32] A. Bhatia, R. Kumar, O.P. Katare, Tamoxifen in topical liposomes: development, characterization and *in vitro* evaluation, J Pharm Pharm Sci 7 (2004) 252–259.
[33] A.R. Mohammed, N. Weston, A.G. Coombes, et al., Liposome formulation of poorly water soluble drugs: optimization of drug loading and ESEM analysis of stability, Int. J. Pharm. 285 (2004) 23–34.
[34] J.A. Zhang, G. Anyarambhatla, L. Ma, et al., Development and characterization of a novel Cremophor® EL free liposome-based paclitaxel (LEP-ETU) formulation, Eur. J. Pharm. Biopharm. 59 (2005) 177–187.
[35] W.K. Subczynski, A. Wisniewska, J.J. Yin, et al., Hydrophobic barriers of lipid bilayer-membranes formed by reduction of water penetration by alkyl chain unsaturation and cholesterol, Biochemistry 33 (1994) 7670–7681.
[36] R. Jangde, D. Singh, Preparation and optimization of Quercetin-loaded liposomes for wound healing, using response surface methodology, Artif. Cells, Nanomed. Biotechnol. 44 (2016) 635–641.
[37] Z.P. Yuan, L.J. Chen, L.Y. Fan, et al., Liposomal Quercetin efficiently suppresses growth of solid tumors in murine models, Clin. Cancer Res. 12 (2006) 3193–3199.
[38] Z. Arsov, L. Quaroni, Direct interaction between cholesterol and phosphatidylcholines in hydrated membranes revealed by ATR-FTIR spectroscopy, Chem. Phys. Lipids 150 (2007) 35–48.
[39] H. Maeda, The enhanced permeability and retention (EPR) effect in tumor vasculature: the key role of tumor-selective macromolecular drug targeting, Adv Enzyme Regul 41 (2001) 189–207.
[40] R. Abbasalipourkabir, A. Salehzadeh, R. Abdullah, Tamoxifen-loaded solid lipid nanoparticles-induced apoptosis in breast cancer cell lines, J. Exp. Nanosci. 11 (2016) 161–174.
[41] D. Kalyane, N. Raval, R. Maheshwari, et al., Employment of enhanced permeability and retention effect (EPR): nanoparticle-based precision tools for targeting of therapeutic and diagnostic agent in cancer, Mater Sci Eng C Mater Biol Appl 98 (2019) 1252–1276.
[42] Z.P. Chen, J.B. Schell, C.-T. Ho, et al., Green tea epigallocatechin gallate shows a pronounced growth inhibitory effect on cancerous cells but not on their normal counterparts, Cancer Lett. 129 (1998) 173–179.
[43] K. Brusselmans, E. De Schrijver, W. Heyns, et al., Epigallocatechin-3-gallate is a potent natural inhibitor of fatty acid synthase in intact cells and selectively induces apoptosis in prostate cancer cells, Int. J. Cancer 106 (2023) 856–862.
[44] J. Cristiano Ceron, N. Rezende, S. Daniela Fernandes, et al., Target selectivity of cholesterol-phosphatidylcholineliposome loaded with phthalocyanine for breastcancer diagnosis and treatment by photodynamictherapy, Photodiagnosis Photodyn. Ther. 39 (2022) 102992.
[45] A. Celine Stoica, Kleber Ferreira, K. Hannan, et al., Bilayer forming phospholipids as targets for cancer therapy, Int J Mol Biosci 23 (2022) 5266.
[46] C. Li, Y. Zhang, Y. Wan, et al., STING-activating drug delivery systems: design strategies and biomedical applications, Chinese Chem Lett 32 (2021) 1615–1625.
[47] H. Zeng, Y. Qi, Z. Zhang, et al., Nanomaterials toward the treatment of Alzheimer's disease: recent advances and future trends, Chinese Chem Lett 32 (2021) 1857–1868.
[48] M. Sun, S. Nie, X. Pan, et al., Quercetin-nanostructured lipid carriers: characteristics and anti-breast cancer activities in vitro, Colloids Surf. B Biointerfaces 113 (2014) 15–24.
[49] A. Jain, N.K. Garg, A. Jain, et al., A synergistic approach of adapalene-loaded nanostructured lipid carriers, and vitamin C coadministration for treating acne, Drug Dev. Ind. Pharm. 42 (2016) 897–905.